

## ADAPTIVE SLIDING MODE CONTROL WITH NON-INTEGGER ORDER REFERENCE FUNCTION

C. Ionescu<sup>1</sup>, C. Copot<sup>1</sup>, A. Chevalier<sup>1</sup>, D. Copot<sup>1</sup> and R. De Keyser<sup>1</sup>

<sup>1</sup>*Ghent University, Department of Electrical energy, Systems and Automation, Technologiepark 914, 9052 Zwijnaarde, Belgium*

**Abstract** — This paper presents a sliding mode control strategy suitable for mechanical sub-systems with varying trajectory dynamics. An illustrative example of a two link robot actuator/manipulator is used. The non-integer order function is introduced in the setpoint definition as to represent changes in the desired trajectory of this sub-system, as well as being used to adapt the control law to the new dynamics. Uncertainties are introduced in the model used for the control law, hence robustness is tested.

**Keywords:** sliding mode control, robot arm, non-integer function, fractional calculus, adaptation

### I – Introduction

Typical two link robot manipulators are often found in heavy duty industry, e.g. automotive assembly lines, agricultural harvesting machines [1]. Due to varying product specification the reference trajectory may change dynamics and amplitude and calibration of the system along with re-tuning controller parameters are necessary to maintain optimal operation [2]. Often these systems are in fact part of complex processes, where sub-system interaction is present and safe operation must be ensured at all times by adapting the reference trajectory.

Another class of applications where reference trajectory may change dynamics and amplitude is that of spacecraft dynamics and spacecraft rendez-vous. Orbital coordinates may be required to adapt to other values due to unexpected space drifts and winds, or obstacle avoidance maneuver.

Medical applications such as radiotherapy for lung tumours also make use of robot link manipulators for positioning laser beam or near infra-red spectroscopy [3]. While at rest, the patient breaths during the treatment, hence the tumour changes position and shape along with the lung tissue [4]. This requires adaptation of the reference trajectory of the beam and accurate position control is of utmost importance.

A nice retrospective with the pioneers of fractional calculus is given in [5]. A comprehensive overview of applications of fractional order control is given in [6]. Discussion on stability in relay controlled systems is made in [7]. Gain adaptation in fractional order control has been discussed in [8]. A practical approach to implementing a fractional order control in a PLC for industrial use has been discussed in [9]. Design of sliding mode controllers for a class of fractional order chaotic systems has been proposed in [10]. The systems under analysis were the fractional-order Chen system,

the fractional order Lorenz system and a fractional order financial system. Numerical simulations supported the effectiveness of the proposed method. On the other hand, fractional order sliding mode controller with terminal convergence bound was proposed for a class of dynamical systems with uncertainty in [11]. There the switching law contains fractional order differential operators and ensures finite stability of the closed loop system.

The present paper proposes a sliding mode control algorithm in which varying reference trajectories are defined using fractional order dynamics. This information is used in the tuning of the control laws and simulation examples illustrate the effectiveness of the proposed methodology for this class of applications.

### II – Model description

Consider an  $n$ -joint robot as follows:

$$\mathbf{H}(\mathbf{q})\ddot{\mathbf{q}} + \mathbf{C}(\mathbf{q}, \dot{\mathbf{q}})\dot{\mathbf{q}} + \mathbf{G}(\mathbf{q}) + \mathbf{F}(\dot{\mathbf{q}}) + \boldsymbol{\tau}_d = \boldsymbol{\tau} \quad (1)$$

where  $\mathbf{q} \in \mathbf{R}^n$  is the angle vector,  $\mathbf{H}(\mathbf{q}) \in \mathbf{R}^{n \times n}$  is the inertia matrix,  $\mathbf{C}(\mathbf{q}, \dot{\mathbf{q}}) \in \mathbf{R}^n$  denotes the centrifugal and coriolis forces,  $\mathbf{G}(\mathbf{q}) \in \mathbf{R}^n$  is the gravity,  $\mathbf{F}(\dot{\mathbf{q}}) \in \mathbf{R}^n$  is the frictional force,  $\boldsymbol{\tau} \in \mathbf{R}^n$  is the control moment, and  $\boldsymbol{\tau}_d \in \mathbf{R}^n$  is the disturbance moment.

The characteristics of the kinetic model are [1]:

- the kinetic model contains a higher number of elements and this depends on the number of robot joints;
- the model has a high degree of nonlinearity;
- there exists a strong interaction between the various sub-systems (i.e. joints);
- there exists model uncertainty and varying dynamics; these depend on the load and joint friction.

Properties of the model defined in 1 [1, 12]:

- $\mathbf{H}(\mathbf{q})$  is a positive-definite symmetrical and bounded matrix; i.e.  $m_1 \mathbf{I} \leq \mathbf{H}(\mathbf{q}) \leq m_2 \mathbf{I}$
- $\mathbf{C}(\mathbf{q}, \dot{\mathbf{q}})$  is bounded, i.e.  $\|\mathbf{C}(\mathbf{q}, \dot{\mathbf{q}})\| \leq c_b(\mathbf{q}) \|\dot{\mathbf{q}}\|$
- matrix  $\dot{\mathbf{H}} - 2\mathbf{C}$  is a skew-symmetric matrix, i.e.  $\mathbf{x}^T (\dot{\mathbf{H}} - 2\mathbf{C})\mathbf{x} = 0$ , with  $\mathbf{x}$  a vector
- the measurable (known) disturbance is bounded by a positive constant  $\|\boldsymbol{\tau}_d\| \leq \tau_M$

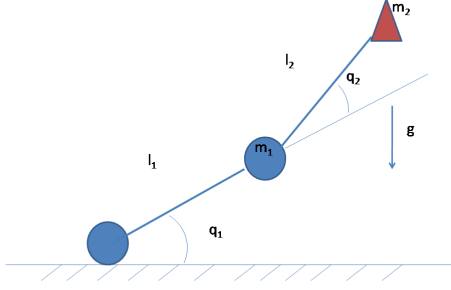


Figure 1: Schematic representation of the robot's last two links. See text for notations.

The illustrative example used in this paper is given by a two joint robot manipulator. This is well in agreement with the real-life cases where position control is mainly achieved by accurate control of the last two joints, as in figure 1.

As a real-life example, the radiotherapy of lung tumours are making use of Cyberknife robot to radiate the tumour tissue. During breathing, the spatial and volumetric shape of the tumour tissue is changing. The breathing period at rest of a patient diagnosed with lung disease is between 0.5-1 Hz (as opposed to a healthy patient, whose breathing period is around 0.3 Hz at rest). Since the changes in amplitude position are very small, it is not necessary to control the position of the robot arm in all its joints. Hence, only the last two joints are used and the model for control is simplified.

The kinetic equation is simplified to:

$$\mathbf{H}(\mathbf{q})\ddot{\mathbf{q}} + \mathbf{C}(\mathbf{q}, \dot{\mathbf{q}})\dot{\mathbf{q}} + \mathbf{G}(\mathbf{q}) = \boldsymbol{\tau} \quad (2)$$

where  $\mathbf{q} = [q_1 \ q_2]$ ,  $\boldsymbol{\tau} = [\tau_1 \ \tau_2]^T$  and

$$\mathbf{H} = \begin{bmatrix} \alpha + 2\varepsilon \cos(q_2) + 2\eta \sin(q_2) & \beta + \varepsilon \cos(q_2) + \eta \sin(q_2) \\ \beta + \varepsilon \cos(q_2) + \eta \sin(q_2) & \beta \end{bmatrix} \quad (3)$$

$$\mathbf{C} = \begin{bmatrix} (-2\varepsilon \sin(q_2) + 2\eta \cos(q_2))\dot{q}_2 & (-\varepsilon \sin(q_2) + \eta \cos(q_2))\dot{q}_2 \\ (\varepsilon \sin(q_2) - \eta \cos(q_2))\dot{q}_1 & 0 \end{bmatrix} \quad (4)$$

$$\mathbf{G} = \begin{bmatrix} \varepsilon e_2 \cos(q_1 + q_2) + \eta e_2 \sin(q_1 + q_2) + (\alpha - \beta + e_1)e_2 \cos(q_1) \\ \varepsilon e_2 \cos(q_1 + q_2) + \eta e_2 \sin(q_1 + q_2) \end{bmatrix} \quad (5)$$

where  $\alpha$ ,  $\beta$ ,  $\varepsilon$  and  $\eta$  are constants, with  $\alpha = I_1 + m_1 l_{c1}^2 + I_e + m_e l_{ce}^2 + m_e l_1^2$ ,  $\beta = I_e + m_e l_{ce}^2$ ,  $\varepsilon = m_e l_1 l_{ce} \cos(\delta_e)$ ,  $\eta = m_e l_1 l_{ce} \sin(\delta_e)$ . The numerical values of the robot joint elements are taken as:

$$\begin{matrix} m_1 = 1\text{kg} & l_1 = 1\text{m} & l_{c1} = 1/2\text{m} & I_1 = 1/12\text{kg} & m_e = 3\text{kg} \\ l_{ce} = 1\text{m} & I_e = 2/5\text{kg} & \delta_e = 0 & e_1 = -7/12 & e_2 = 9.81 \end{matrix} \quad (6)$$

Let  $\mathbf{a} = [\alpha \ \beta \ \varepsilon \ \eta]^T$  and  $\hat{\mathbf{a}}$  its estimated values. We assume  $\dot{\hat{\mathbf{a}}} = \hat{\mathbf{a}} - \mathbf{a}$  since  $\mathbf{a}$  is a constant vector and thus  $\dot{\hat{\mathbf{a}}} = \hat{\mathbf{a}}$ . This implies that we can estimate the matrices  $\hat{\mathbf{H}}$ ,  $\hat{\mathbf{C}}$  and  $\hat{\mathbf{G}}$ , respectively.

For our system, we do not know the values of  $\mathbf{a}$ . Denote by  $\mathbf{q}_d$  the desired reference trajectory. The tracking error is given by:

$$\mathbf{e} = \mathbf{q}_d - \mathbf{q} \quad (7)$$

Define

$$\dot{\mathbf{q}}_r = \dot{\mathbf{q}}_d + \Lambda(\mathbf{q}_d - \mathbf{q}) \quad (8)$$

with  $\Lambda$  a positive diagonal matrix. In this relation, the terms in  $\mathbf{q}_d$  are important since they define the desired trajectories. In case the sliding surface is not adapted to changes in desired trajectory, this control strategy will have steady state error.

Making use of the dynamic regression matrix formulation from [13, 2], we have that:

$$\mathbf{H}(\mathbf{q})\ddot{\mathbf{q}}_r + \mathbf{C}(\mathbf{q}, \dot{\mathbf{q}}_r)\dot{\mathbf{q}}_r + \mathbf{G}(\mathbf{q}) = \mathbf{Y}(\mathbf{q}, \dot{\mathbf{q}}, \dot{\mathbf{q}}_r, \ddot{\mathbf{q}}_r)\mathbf{a} \quad (9)$$

and

$$\hat{\mathbf{H}}(\mathbf{q})\ddot{\mathbf{q}}_r + \tilde{\mathbf{C}}(\mathbf{q}, \dot{\mathbf{q}}_r)\dot{\mathbf{q}}_r + \tilde{\mathbf{G}}(\mathbf{q}) = \mathbf{Y}(\mathbf{q}, \dot{\mathbf{q}}, \dot{\mathbf{q}}_r, \ddot{\mathbf{q}}_r)\hat{\mathbf{a}} \quad (10)$$

where

$$\mathbf{Y}(\mathbf{q}, \dot{\mathbf{q}}, \dot{\mathbf{q}}_r, \ddot{\mathbf{q}}_r) = \begin{bmatrix} y_{11} & y_{12} & y_{13} & y_{14} \\ y_{21} & y_{22} & y_{23} & y_{24} \end{bmatrix} \quad (11)$$

with

$$y_{11} = \dot{q}_{r1} + e_2 \cos(q_1) \quad (12)$$

$$y_{12} = \dot{q}_{r2} - e_2 \cos(q_1) \quad (13)$$

$$y_{13} = 2 \cos(q_2) \dot{q}_{r1} + \cos(q_2) \dot{q}_{r2} - 2 \sin(q_2) \dot{q}_2 \dot{q}_{r1} - \sin(q_2) \dot{q}_2 \dot{q}_{r2} + e_2 \cos(q_1 + q_2) \quad (14)$$

$$y_{14} = 2 \sin(q_2) \dot{q}_{r1} + \sin(q_2) \dot{q}_{r2} + 2 \cos(q_2) \dot{q}_2 \dot{q}_{r1} + \cos(q_2) \dot{q}_2 \dot{q}_{r2} + e_2 \sin(q_1 + q_2) \quad (15)$$

$$y_{21} = 0; y_{22} = \dot{q}_{r1} + \dot{q}_{r2} \quad (16)$$

$$y_{23} = \cos(q_2) \dot{q}_{r1} + \sin(q_2) \dot{q}_1 \dot{q}_{r1} + e_2 \cos(q_1 + q_2) \quad (17)$$

$$y_{24} = \sin(q_2) \dot{q}_{r1} - \cos(q_2) \dot{q}_1 \dot{q}_{r1} + e_2 \sin(q_1 + q_2) \quad (18)$$

### III – Sliding Mode Control Algorithm

In this paper, we propose the use of classical sliding mode control strategy as briefly introduced in the remainder of this section for the application defined by (9)[13]. The originality of our approach is not in the control algorithm itself, but in the definition of the reference trajectory, consequently used in the controller law.

The sliding variable is given by

$$\mathbf{s} = \dot{\mathbf{e}} + \Lambda \mathbf{e} \quad (19)$$

Notice that changes in the desired reference trajectory  $\mathbf{q}_d$  are taken up via the error term defined earlier in (7). Selecting the Lyapunov function

$$V(t) = \frac{1}{2} \mathbf{s}^T \mathbf{H}(\mathbf{q}) \mathbf{s} \quad (20)$$

we have that

$$\dot{V}(t) = \mathbf{s}^T [\mathbf{H}(\mathbf{q})\ddot{\mathbf{q}}_r + \mathbf{C}(\mathbf{q}, \dot{\mathbf{q}})\dot{\mathbf{q}}_r + \mathbf{G}(\mathbf{q}) - \boldsymbol{\tau}] \quad (21)$$

Hence, we can design the controller law as:

$$\tau = \hat{\mathbf{H}}(\mathbf{q})\ddot{\mathbf{q}}_r + \hat{\mathbf{C}}(\mathbf{q}, \dot{\mathbf{q}})\dot{\mathbf{q}}_r + \hat{\mathbf{G}}(\mathbf{q}) + \tau_s \quad (22)$$

with  $\tau_s$  the design parameter for robustness. Making use of (20) and (21) it follows that:

$$\dot{V}(t) = \mathbf{s}^T [\tilde{\mathbf{H}}(\mathbf{q})\ddot{\mathbf{q}}_r + \tilde{\mathbf{C}}(\mathbf{q}, \dot{\mathbf{q}})\dot{\mathbf{q}}_r + \tilde{\mathbf{G}}(\mathbf{q}) - \tau_s] = \mathbf{s}^T [\mathbf{Y}(\mathbf{q}, \dot{\mathbf{q}}, \ddot{\mathbf{q}}_r, \dot{\mathbf{q}}_r)\tilde{\mathbf{a}} - \tau_s] \quad (23)$$

Selecting

$$\tau_s = \mathbf{k} \text{sgn}(\mathbf{s}) + \mathbf{s} = \begin{bmatrix} k_1 \text{sgn}(s_1) + s_1 \\ k_2 \text{sgn}(s_2) + s_2 \end{bmatrix} \quad (24)$$

where  $k_i = \sum_{j=1}^4 \bar{Y}_{ij} \bar{a}_j$ , with  $i = 1, 2$ . From (23) and (24) we obtain the control law.

Considering the desired reference trajectories as defined by:

$$\begin{aligned} q_{d1} &= \omega^\gamma \sin(\omega^\gamma t) \\ q_{d2} &= \omega^\gamma \sin(\omega^\gamma t) \end{aligned} \quad (25)$$

This implies that if dynamics of the true system (i.e. frequency) are varying in such way that dynamics of  $\gamma$  may be introduced, adaptation is necessary and sufficient to ensure good performance. By estimating the  $\gamma$  values of the desired reference trajectories using a simple iterative algorithm, one can significantly improve the controller performance. This can be done by changing values for  $\gamma$  with small increments/decrements to detect improvements in the performance due to variations in (25). The control law (22) will then adapt the sliding surface via (8) where the desired trajectory is changed according to the new values for  $\gamma$ .

#### IV – Results

In this analysis, assume  $\Lambda = 5 \cdot I$ . To avoid chattering in the control effort, the saturated function is used instead of the switch function with  $\Delta = 0.05$ . The basis frequency is assumed to be  $\omega = 1$  Hz, denoting a breathing frequency of a patient. These parameters do not change from these values in the next simulation tests.

*First*, we test the system assuming we know perfectly the trajectory of the reference, for  $\gamma = 1$ . The results of the closed loop control are given in figure 2 for the two controlled positions and two control efforts.

*Second*, we assume three possible cases:

- when  $\gamma = 0.3$
- when  $\gamma = 0.5$  and
- when  $\gamma = 0.8$

in which the value for  $\gamma$  used in the controller is not known apriori and needs to be estimated online. Uncertainty between model and plant is introduced at 50%. A classical recursive least squares identification algorithm is used in this case. The initial value is set to  $\gamma = 1$ .

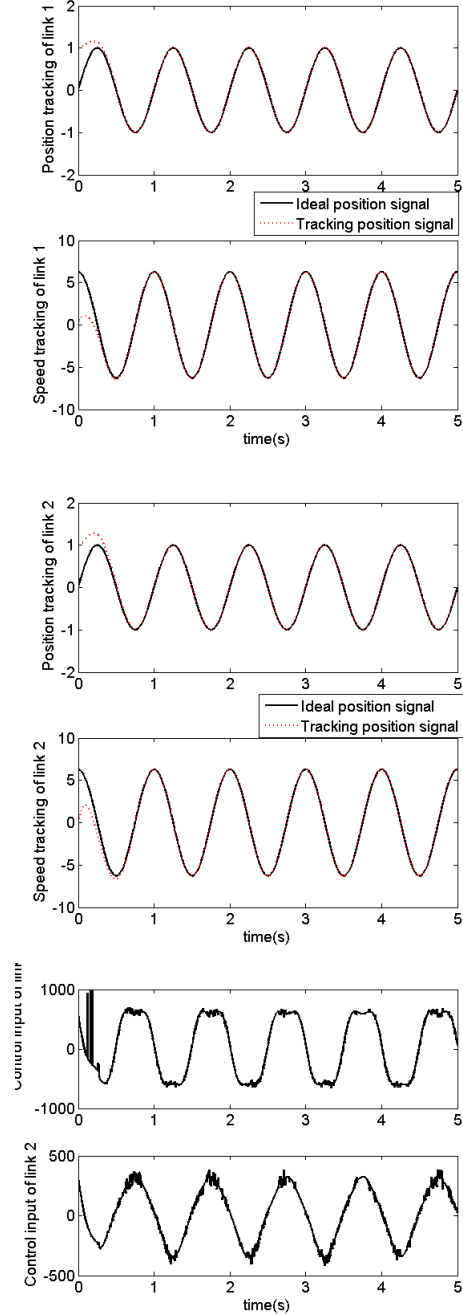


Figure 2: Simulation results for the ideal case when the reference trajectory is perfectly known, with a fractional order variable  $\gamma = 1$ .

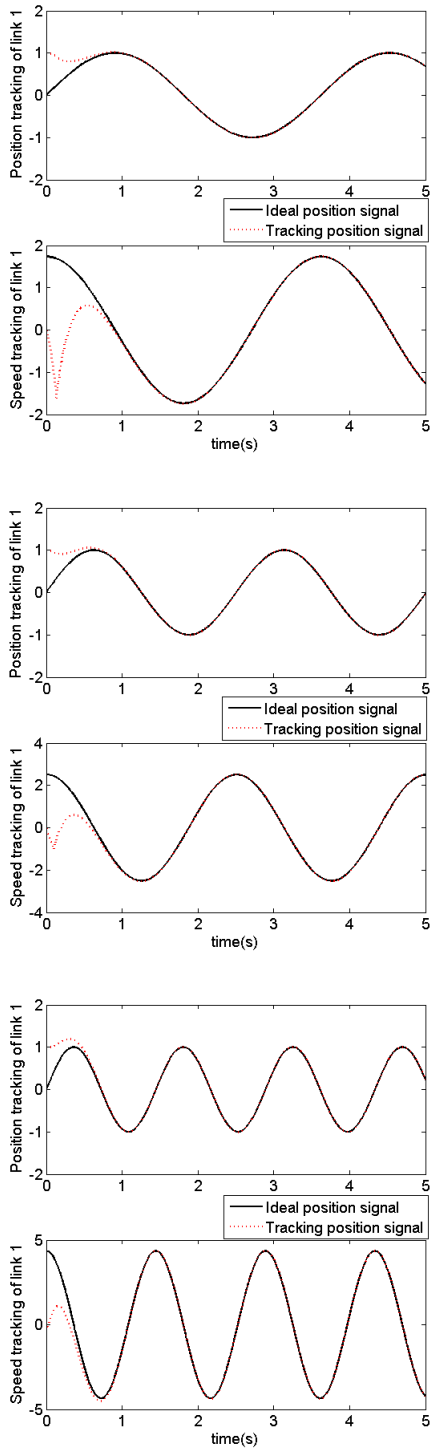


Figure 3: Output of the first joint for various values of the reference signal fractional order variable  $\gamma = 0.3; 0.5; 0.8$  - from top to bottom.

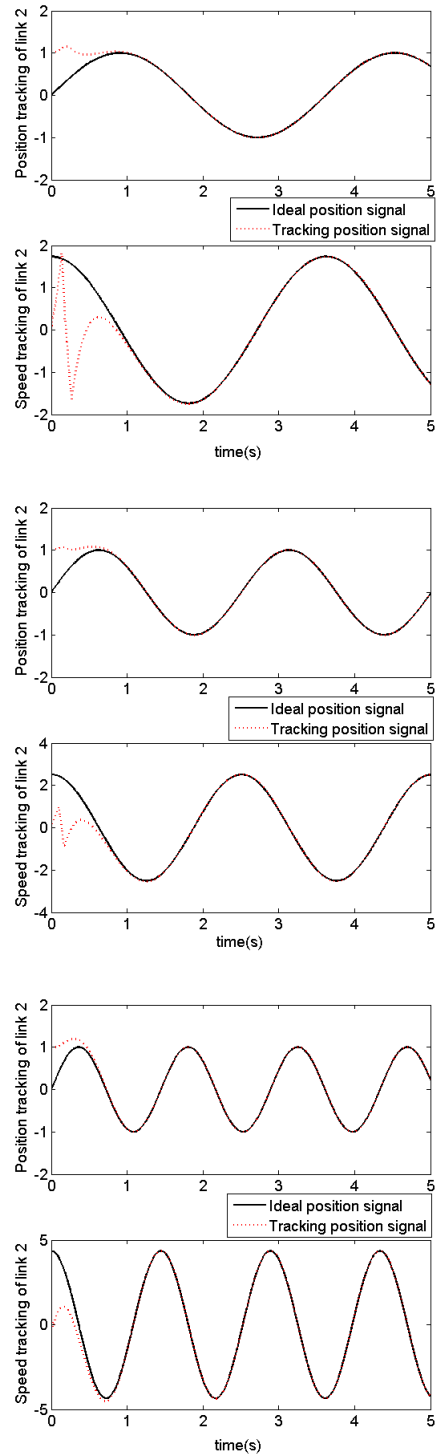


Figure 4: Output of the second joint for various values of the reference signal fractional order variable  $\gamma = 0.3; 0.5; 0.8$  - from top to bottom.

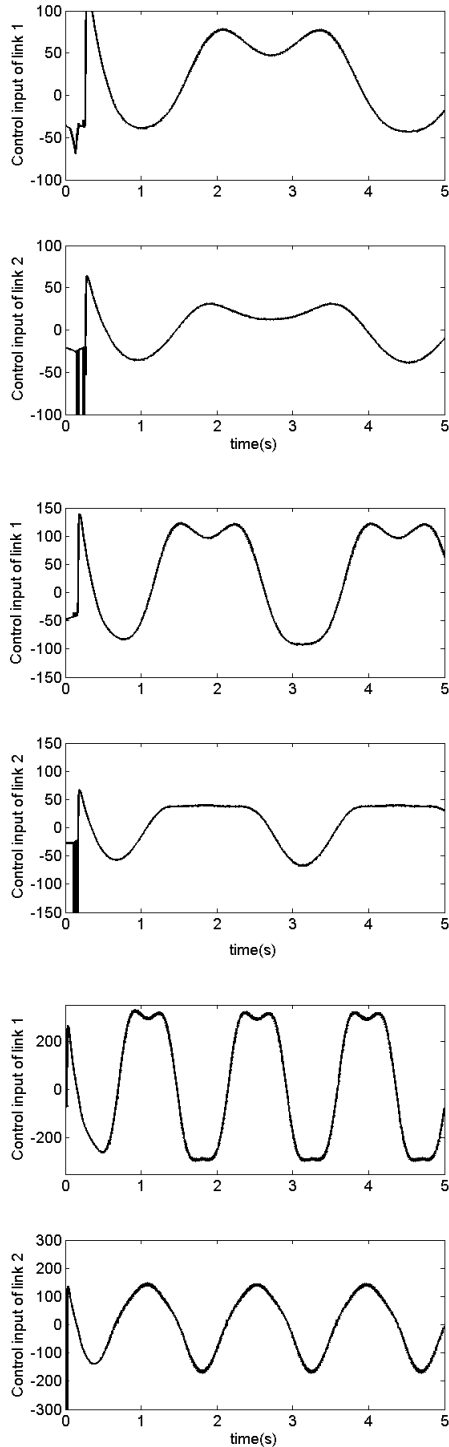


Figure 5: Control effort of the two joints for various values of the reference signal fractional order variable  $\gamma = 0.3; 0.5; 0.8$  - from top to bottom.

The results are given in figure 3 for the output of the first link. Figure 4 depicts the output of the second link. The control effort of the two joints is given in figure 5.

Third, we introduce saturations at  $\pm 500$  mV in the control effort. This is likely to be the case in real-life applications. We want to check the adaptation algorithm for changes in the frequency which introduce modelling errors. At time instant 2.5 seconds the value is changed from 1 to 1.15 Hz. The results for  $\gamma = 0.8$  are given in figure 6. Indeed, it can be observed that now the control output reaches saturation when the change in frequency occurs and the performance slightly deteriorates at the beginning; however, this deterioration is circumvented successfully by the adaptation law in the control algorithm.

It can be observed that under all conditions, the control law is able to follow the reference trajectory which changes due to the changes in the  $\gamma$  values. As expected, the closed loop performance becomes optimal after the correct value for  $\gamma$  has been identified in the model of the controller. Once this is done, then the controller has no difficulty to follow the dynamic reference trajectory.

### V – Conclusion

In this paper, sliding mode control of a dynamic reference trajectory is presented. The example used to illustrate the effectiveness of the control can be widely encountered in industrial and medical applications.

### References

- [1] S. Kawamura and M. Svinin (eds). Springer, 2006.
- [2] J.E. Slotine and W.P. Li. *Int J Rob Res*, 6(3):49–59, 1987.
- [3] T. Neicu, H. Shirato, Y. Seppenwoolde, and S. B Jiang. *Phys. Med. Biol.*, 48:587–598, 2003.
- [4] Y. Seppenwoolde, H. Shirat, K. Kei Kitamura, S. Shimizu, M. van Herk, J. V. Lebesque, and K. Miyasaka. *Int J Rad Onc Biol Physics*, 53(4):822–834, 2002.
- [5] D. Valerio, J.T. Machado, and V. Kiryakova. *FRACTIONAL CALCULUS AND APPLIED ANALYSIS*, 17(2):552–578, 2014.
- [6] M.S. Tavazoei. *FRACTIONAL CALCULUS AND APPLIED ANALYSIS*, 17(2):49–59, 2014.
- [7] R. Caponetto, G. Maione, A. Pisano, M.R. Rapaic, and E. Usai. *FRACTIONAL CALCULUS AND APPLIED ANALYSIS*, 16(1):93–108, 2013.
- [8] I. Tejado and B. Vinagre H. HosseinNia and. *FRACTIONAL CALCULUS AND APPLIED ANALYSIS*, 17(2):462–482, 2014.

- [9] P. Lanusse and J. Sabatier. *FRACTIONAL CALCULUS AND APPLIED ANALYSIS*, 14(4):505–522, 2011.
- [10] C. Yin, S-M Zhong, and W-F Chen. *Comm Non Sci Numer Sim*, 17:356–366, 2012.
- [11] S. Dadras and H. R. Momeni. *Comm Non Sci Numer Sim*, 17:367–377, 2012.
- [12] J.E. Slotine and W.P. Li. Prentice Hall, 1991.
- [13] J. Liu and X. Wang. Springer-Verlag, Berlin Heidelberg, 2012.

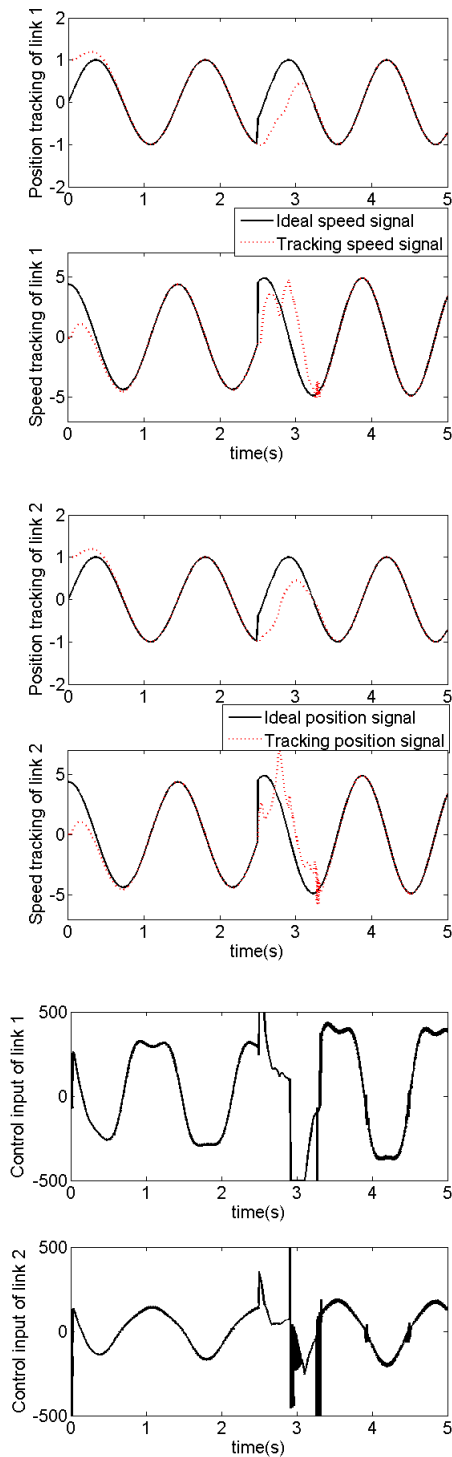


Figure 6: Simulation results for the case when the input to the process is saturated and the frequency changes from 1 to 1.15 at time instant 2.5 seconds.